

Available online at www.sciencedirect.com

ScienceDirect

journal homepage: <http://Elsevier.com/locate/radcr>

Neuroradiology

Biologically aggressive regions within glioblastoma identified by spin-lock contrast T1 relaxation in the rotating frame (T1 ρ) MRI

Ramon Francisco Barajas Jr. MD^{a,b}, Javier Villanueva-Meyer MD^c, Arie Perry MD^d, Mitchel Berger MD^e, Soonmee Cha MD^{c,e,*}

^a Department of Radiology, Oregon Health and Science University, Portland, OR

^b Advanced Imaging Research Center, Oregon Health and Science University, Portland, OR

^c Department of Radiology and Biomedical Imaging, University of California San Francisco, 350 Parnassus Avenue, San Francisco, CA 94117

^d Department of Pathology and Laboratory Medicine, University of California San Francisco, San Francisco, CA

^e Department of Neurological Surgery, University of California San Francisco, 350 Parnassus Avenue, San Francisco, CA 94117

ARTICLE INFO

Article history:

Received 2 June 2017

Received in revised form 12 June 2017

Accepted 3 July 2017

Available online

Keywords:

Glioblastoma

Glioma

T1 ρ MRI

T1rho MRI

Spin-lock contrast

Image-guided

ABSTRACT

Spin-lattice relaxation in the rotating frame magnetic resonance imaging allows for the quantitative assessment of spin-lock contrast within tissues. We describe the utility of spin-lattice relaxation in the rotating frame metrics in characterizing glioblastoma biological heterogeneity. A 84-year-old man presented to our institution with a right frontal temporal mass. Prior tissue sampling from a peripheral nonenhancing lesion was nondiagnostic. Stereotactic image-guided tissue sampling of the nonenhancing T2-fluid-attenuated inversion recovery hyperintense region involving the anterior cingulate gyrus with elevated spin-lattice relaxation in the rotating frame metrics provided a pathologic diagnosis of glioblastoma. This case illustrates the utility of spin-lattice relaxation in the rotating frame magnetic resonance imaging in identifying biologically aggressive regions within glioblastoma.

© 2017 the Authors. Published by Elsevier Inc. under copyright license from the University of Washington. This is an open access article under the CC BY-NC-ND license (<http://creativecommons.org/licenses/by-nc-nd/4.0/>).

Introduction

Glioma is the most common supratentorial brain tumor affecting approximately 138,000 individuals in the United States

in 2010, with an annual incidence of 17,000 new cases [1]. Despite significant advances in surgical, radiation, and medical therapies, the prognosis of this disease remains dismal, with a median survival of less than 2 years for the most malignant form, glioblastoma [2]. A number of biological, clinical,

Acknowledgments: This work was funded by grant number 5T32EB001631-07 from the National Institutes of Health Roadmap for Medical Research. The first author thanks Bethany Barajas for her helpful comments regarding this manuscript.

Competing Interests: The authors have declared that no competing interests exist.

* Corresponding author.

E-mail address: Soonmee.Cha@ucsf.edu (S. Cha).

<https://doi.org/10.1016/j.radcr.2017.07.010>

1930-0433/© 2017 the Authors. Published by Elsevier Inc. under copyright license from the University of Washington. This is an open access article under the CC BY-NC-ND license (<http://creativecommons.org/licenses/by-nc-nd/4.0/>).

and diagnostic factors account for the poor prognostic outcomes of patients with glioma. One factor that directly impacts the diagnosis of glioma is tumoral biological heterogeneity.

The pathologic assessment of glioma relies on an invasive procedure for tissue sampling that is often performed without regard for tumor biological heterogeneity. The assessment of tumor aggressiveness based on isolated regional tissue samples can lead to sampling error, resulting in undergrading, with a published report in up to 30% of cases [3,4]. The inherent limitations of histologic techniques to assess tumor grade have led to the development of imaging-based methods for the noninvasive quantification of aggressive biological characteristics.

Recent advances in magnetic resonance imaging (MRI) have provided for the acquisition of physiological metrics with the potential to noninvasively assess biological characteristics that influence the tumor grade and the clinical prognosis of patients with glioma. These physiological MRI sequences contribute data that complement the standard information provided by traditional morphologic T1- and T2-weighted techniques. One recently developed physiological sequence is spin-lattice relaxation in the rotating frame (T1 ρ). T1 ρ allows for the quantitative assessment of spin-lock contrast within tissues [5]. Aronen et al. have previously published a case series of T1 ρ imaging obtained at 0.1-T field strength in a cohort of 11 patients with high-grade glioma and concluded that spin-lock contrast maps have the potential to improve tissue biological characterization. Therefore, the specific aim of this case report was to describe our initial experience with the use of T1 ρ MRI in characterizing glioblastoma biological heterogeneity.

Case report

An 84-year-old man presented to our institution on April 2014 with a right frontal temporal mass lesion (Fig. 1). Relevant past medical history included adenocarcinoma of the left lung, for which the patient had undergone lobectomy on August 2013.

On September 2013, the patient experienced a brief episode of vertigo that resulted in a fall from standing. MRI of the brain demonstrated a nonenhancing T2 hyperintense mass centered within the right frontal operculum with regional extension including the anterior cingulate gyrus. The patient underwent a short-interval follow-up MRI on October 2013 that was unchanged. Imaging on March 2014 demonstrated a progression of a presumed, but not pathologically confirmed, glioma evidenced by focal contrast enhancement, now within the orbitofrontal gyri. At another institution, the patient underwent burr hole tissue sampling from within the peripheral nonenhancing margin involving the superior frontal gyrus white matter. The lack of infiltrative tumor cells resulted in the sample being classified as nondiagnostic (Fig. 2, center left image).

On April 2014, the patient presented to our institution's Neurological Surgery service for image-guided tissue sampling and subsequent therapy. Standard preoperative MRI using a 3.0-T scanner (Discovery; GE Healthcare, Waukesha, WI) was obtained 24 hours before the tissue sampling procedure ([6–8]; Fig. 1 and Fig. 2).

A magnetization-prepared 3-dimensional pseudo-steady-state fast spin-echo acquisition pulse sequence was used for T1 ρ quantification. T1 ρ imaging parameters included 0.9 × 0.9 × 1.6 mm resolution, 280 × 196 mm field of view, 120 slices, 0.5 number of excitations, 2× Autocalibrating Reconstruction for Cartesian parallel imaging (GE Healthcare) along the phase encoding direction, an echo train length of 132, a spin-lock frequency of 500 Hz, and a time of spin lock of 2, 10, 40, 60, 80, and 100 ms. The total scan time for T1 ρ data acquisition was 3.5 minutes. T1 ρ imaging was performed before the intravenous administration of 0.1 mmol/kg gadopentetate dimeglumine (Gd-DTPA; Magnevist, Bayer HealthCare Pharmaceuticals).

T1 ρ image processing was performed offline using a commercially available postprocessing workstation (Advantage Workstation, GE Healthcare) and software (FuncTool 9.4.05a, GE Healthcare), allowing for the generation of quantitative whole-brain spin-lock contrast maps (Fig. 1 and Fig. 2) that could

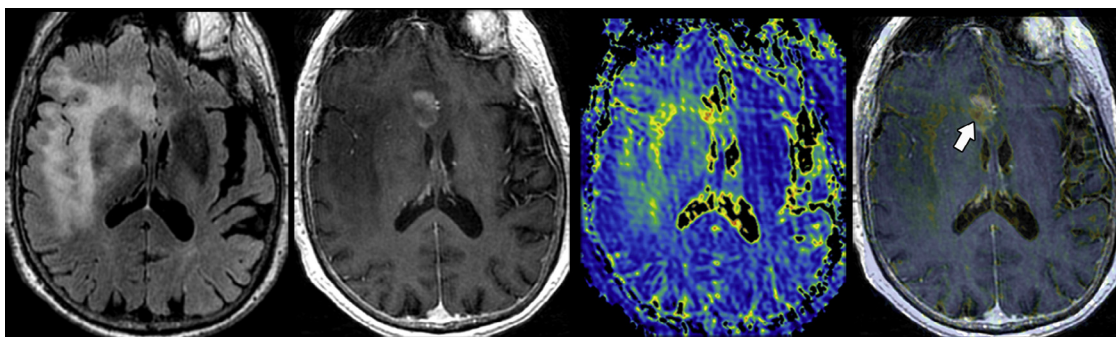


Fig. 1 – Preoperative MRI of a right frontal temporal mass lesion. An 84-year-old man presented to our institution with a T2/FLAIR hyperintense mass (left image) within the right frontal operculum with extension into the right subinsular white matter, anterior cingulate, right anterior temporal, and mesotemporal lobes. Focal contrast enhancement (center left image) was observed within the right cingulate gyrus. Despite the patient's past medical history of lung adenocarcinoma, the morphologic appearance of the mass was believed to be likely due to a high-grade primary glial neoplasm. T1 ρ MRI (center right image) demonstrates heterogeneous spin-lock contrast values within the enhancing and nonenhancing tumor components. Fused T1 ρ and T1-weighted postcontrast image (right image) demonstrates a focal region of markedly elevated T1 ρ within a nonenhancing tumor component (arrow). MRI, magnetic resonance imaging.

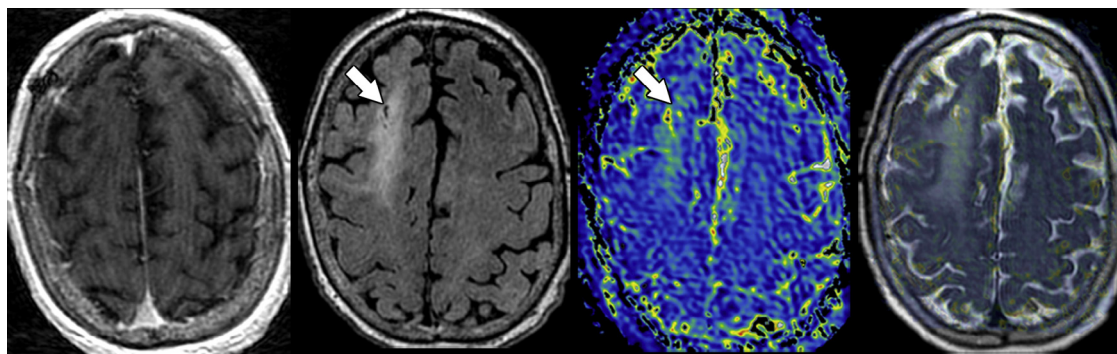


Fig. 2 – Site of nondiagnostic tissue sampling demonstrates a minimally increased $T1\rho$. Stereotactic magnetic resonance-guided tissue sampling (arrows) from a nonenhancing (left) T2-fluid-attenuated inversion recovery hyperintense (center left) component of the mass within the superior frontal gyrus white matter 1 month prior yielded a nondiagnostic pathologic result. $T1\rho$ magnetic resonance imaging (center right) demonstrated fairly homogenous, minimally elevated, spin-lock contrast values. Fused (right) $T1\rho$ and fluid-attenuated inversion recovery weighted imaging shows the previously sampled portion of the tumor is from within a region of minimally elevated $T1\rho$ when compared to the contralateral normal-appearing white matter.

be integrated into the stereotactic image-guided procedure (Brainlab, VectorVision Navigation System).

Anatomic and physiological MRI was used to guide the prospective selection of tissue sampling sites felt most likely to represent a bulk tumor that would allow for a definitive diagnosis of disease etiology. Two sampling sites were preoperatively planned utilizing the surgical navigation workstation (Brainlab, VectorVision Navigation System). Criteria used to plan sites were based upon results from previous studies as having either a relative cerebral blood volume of >3 , an apparent diffusion coefficient of <1200 , and a Cho to N-acetyl aspartate index of >2.0 ; however, this provided for only a

target within the subinsular white matter that was not radially accessible by a right transfrontal stereotactic approach [8,9]. Tissue sampling was performed as close to the target of interest yielding a single diagnostic sample (Fig. 3). A retrospective evaluation of the $T1\rho$ map demonstrated a nonenhancing region within the anterior cingulate with markedly elevated spin-lock contrast metrics ($T1\rho_{\min} = 110$, $T1\rho_{\text{mean}} = 244$, $T1\rho_{\max} = 352$) above background normal-appearing white matter (NAWM; $T1\rho_{\min} = 62$, $T1\rho_{\text{mean}} = 89$, $T1\rho_{\max} = 126$). Relative $T1\rho$ values within the anterior cingulate gyrus were calculated as the ratio of the lesion to the NAWM ($rT1\rho_{\min} = 1.77$, $rT1\rho_{\text{mean}} = 2.74$, $rT1\rho_{\max} = 2.79$).

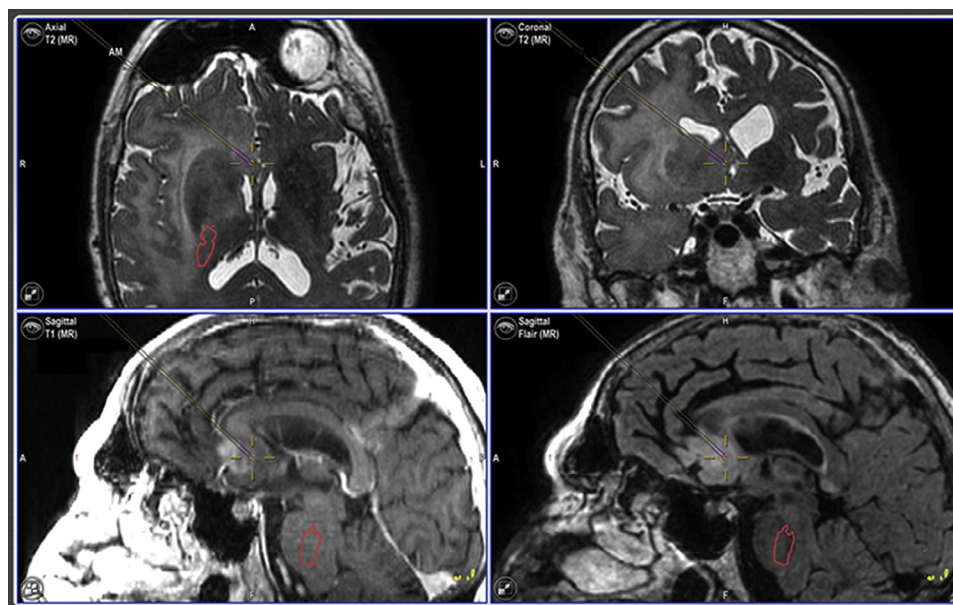


Fig. 3 – Image-guided tissue sampling of a nonenhancing focus provides a pathologic diagnosis of glioblastoma. Intraoperative screenshot obtained at the time of magnetic resonance-guided tissue sampling from a nonenhancing component of the tumor within the anterior cingulate gyrus demonstrates the location of the diagnostic tissue specimen (purple bars centered in cross hair).

Interrogation of the T2 hyperintense nonenhancing white matter adjacent to the prior nondiagnostic tissue sampling site within the right superior frontal gyrus demonstrated lesion T1 ρ values (T1 ρ_{\min} = 102, T1 ρ_{mean} = 126, T1 ρ_{\max} = 165) that were only mildly elevated with respect to NAWM (T1 ρ_{\min} = 59, T1 ρ_{mean} = 85, T1 ρ_{\max} = 122) (Fig. 2). This finding provided for rT1 ρ values that were less than the similar-appearing nonenhancing T2 hyperintense lesion within the anterior cingulate gyrus (rT1 ρ_{\min} = 1.73, rT1 ρ_{mean} = 1.48, rT1 ρ_{\max} = 1.35) (Fig. 4).

Intraoperative stereotactic magnetic resonance-guided tissue sampling of the nonenhancing T2-fluid-attenuated inversion recovery hyperintense region involving the anterior cingulate gyrus with elevated T1 ρ metrics provided a pathologic diagnosis of glioblastoma with a Ki-67 score of 40% (Fig. 5). Given the high diagnostic yield of this tissue sample, no additional samples were obtained. The patient subsequently recovered well from the procedure and was discharged on postoperative day 5. Surgical debulking of the tumor was not performed because of the extent and the location of the disease. The patient is currently undergoing radiotherapy (2 Gy/day, 5 days/week for 6 weeks, total dose of 60 Gy) and

temozolomide-based medical therapy (75 mg/m²/day for 42 days followed by 150 mg/m²/day for 5 consecutive days over 28 days for 6 cycles).

Discussion

This case report highlights our initial experience in using T1 ρ MRI to differentiate similar-appearing nonenhancing regions of T2 hyperintensity caused by a biologically aggressive glioblastoma from regions of non-tumor infiltrated vasogenic edema. The nonenhancing tissue sampling site comprising vasogenic edema without tumor demonstrated T1 ρ values that were only slightly elevated from NAWM (Fig. 3). Conversely, the nonenhancing tissue sampling site comprising glioblastoma had mean and maximum T1 ρ values almost 3fold higher than NAWM. To our knowledge, this is the first report of T1 ρ MRI directly characterizing an aggressive biological process heterogeneously occurring within a patient with glioblastoma. We provide pathologic confirmation that T1 ρ imaging differs regionally within glioblastoma when compared to reactive white matter changes resulting from vasogenic edema.

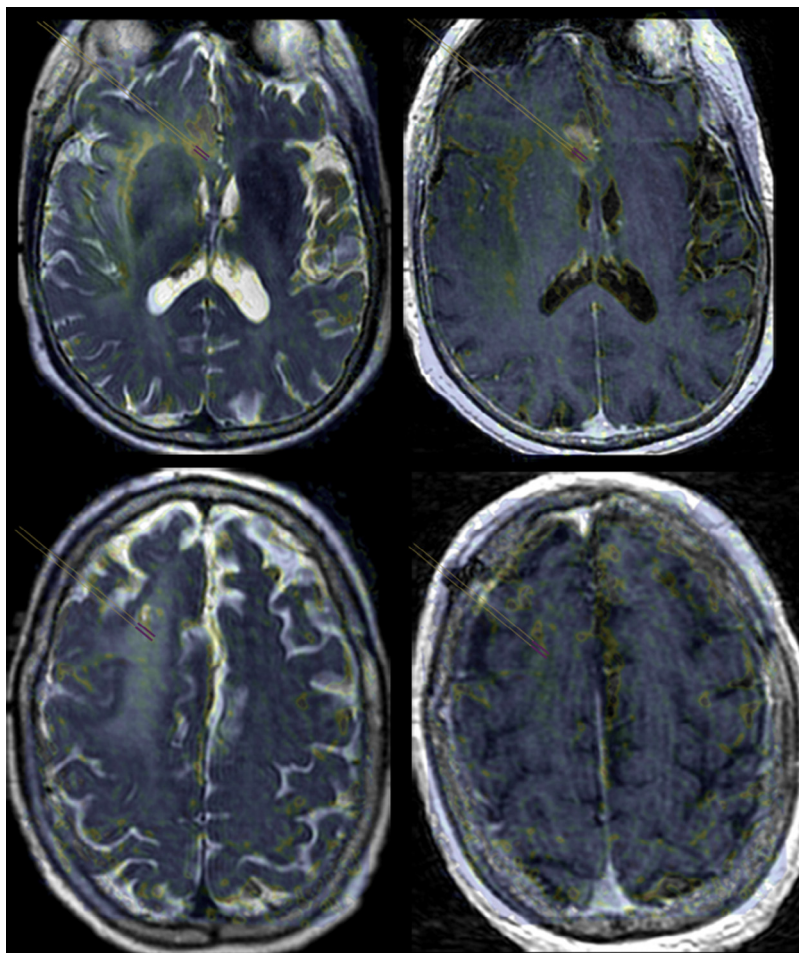


Fig. 4 – Fusion of T1 ρ and morphologic magnetic resonance imaging allows for spin-lock contrast quantification. Fusion of the region of interest (purple bars) placed on a T1 ρ spin-lock contrast map that has been fused to T2 (left) and T1 postcontrast (right) images allows for quantification of T1 ρ metrics within the nonenhancing tissue sampling sites from diagnostic (top) and nondiagnostic (bottom) regions.

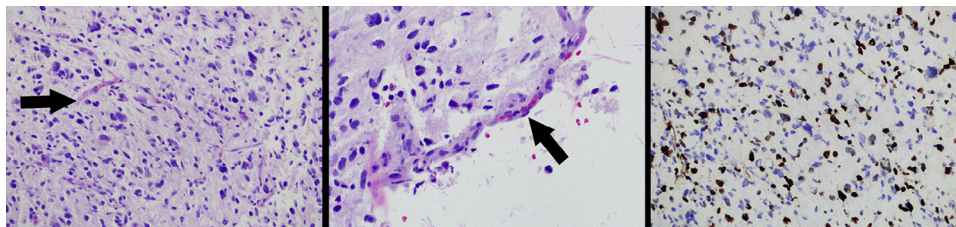


Fig. 5 – Histologic analysis of tissue specimen obtained from within the anterior cingulate gyrus. Hematoxylin and eosin stain (left and middle) and Ki-67 (right) images of a tissue specimen obtained from within a nonenhancing T2 hyperintense tumor component with markedly elevated T1 ρ metrics (Figs. 1, 2 and 4) demonstrates microvascular proliferation (arrows) and a markedly increased cellular proliferation (brown-stained cells) characteristic of biologically aggressive features diagnostic of glioblastoma.

T1 ρ was initially described within solid-state materials by Redfield [10,11]. To date, clinical applications of this MRI technique has been most widely applied to evaluating the hydration status of human articular cartilage. However, the neurologic applications of T1 ρ MRI have been explored in patients with ischemia, neurodegenerative disorders, and brain tumors, and as a response assessment to gene therapy within glioma mouse models [12–23]. T1 ρ MRI obtains tissue contrast through the quantification of spin-lattice relaxation in the rotating frame. This technique allows for the measurement of low-frequency processes at clinical MRI field strengths [24,25]. This measurement is achieved by first flipping the spin magnetization into the transverse plane by a 90° radiofrequency pulse. Next, a spin-lock pulse (low-powered B₁ radiofrequency pulse) is applied parallel to the magnetic moment. The spin-locked magnetization then relaxes with a time constant T1 ρ during the application of the spin-lock pulse. T1 ρ dispersion is then measured by varying the B₁ field amplitude within a constant B₀ field. This technique allows for the measurement of spin interaction and motional processes that occur at very low frequency components (100 Hz to a few kilohertz).

The biological etiology of differential T1 ρ relaxation within glioma has not been fully adjudicated; however, proton chemical exchange (pH), dipole-dipole interactions, spin-spin coupling, diffusion, and slow rotational motions of spins on large macromolecules have been postulated to contribute in various degrees [26]. Histologically, within cartilage specimens, variation in the T1 ρ relaxation is hypothesized primarily to be due to the hydration status and the interaction between the restricted water pool and the free water pool [27].

Within glioma, we hypothesize that variation in T1 ρ relaxation is similarly related to the interaction between free and bound water molecules. The observation of elevated T1 ρ associated with biologically aggressive glioblastoma tissues may be multifactorial; however, a predominating factor may be due to the degree of vasogenic edema. Within glioblastoma, a hypoxia-mediated vascular endothelial growth factor expression has been shown to upregulate neovascularization [28]. This results in deregulated angiogenesis, endothelial proliferation, and increased capillary permeability. The increase in local capillary endothelial permeability results in an immediate increase in the interstitial nutrient supply that facilitates tumor growth. However, this also results in interstitial hydration (vasogenic edema) manifested by T2/FLAIR prolongation on MRI. The tissue contrast provided by T1 ρ imaging may provide a

quantifiable map of tissue hydration status not possible by FLAIR or T2-weighted sequences. Future applications of T1 ρ imaging could include reducing tissue sampling error and undergrading within nonenhancing gliomas.

The observations of this case report are inherently limited. Further prospective studies adjudicating the biological influences and clinical significance of T1 ρ MRI in patients diagnosed with glioma are needed. One possible obstacle to overcome with T1 ρ imaging is its propensity to cause tissue heating. Prior studies have suggested the high specific absorption rate that occurs during prolonged spin-lock pulses may be an impediment to the widespread clinical application of T1 ρ MRI [29,30]. We have decreased the likelihood of tissue heating by limiting the spin-lock time to a maximum of 100 ms.

Conclusion

The observations of this case report suggest that it is feasible to integrate T1 ρ MRI into the clinical evaluation for biologically aggressive regions within glioblastomas.

REFERENCES

- [1] Porter KR, McCarthy BJ, Freels S, Kim Y, Davis FG. Prevalence estimates for primary brain tumors in the United States by age, gender, behavior, and histology. *Neuro Oncol* 2010;12(6):520–7.
- [2] Omuro A, DeAngelis LM. Glioblastoma and other malignant gliomas: a clinical review. *JAMA* 2013;310(17):1842–50.
- [3] Prayson RA, Agamanolis DP, Cohen ML. Interobserver reproducibility among neuropathologists and surgical pathologists in fibrillary astrocytoma grading. *J Neurol Sci* 2000;175:33–9.
- [4] Coons SW, Johnson PC, Scheithauer BW, Yates AJ, Pearl DK. Improving diagnostic accuracy and interobserver concordance in the classification and grading of primary gliomas. *Cancer* 1997;79:1381–93.
- [5] Rommel E, Kimmich R. T1 rho dispersion imaging and volume-selective T1 rho dispersion weighted NMR spectroscopy. *Magn Reson Med* 1989;12:390–9.
- [6] McKnight TR, Smith KJ, Chu PW, Chiu KS, Cloyd CP, Chang SM, et al. Choline metabolism, proliferation, and angiogenesis in nonenhancing grades 2 and 3 astrocytoma. *J Magn Reson Imaging* 2011;33(4):808–16.

- [7] Khayal IS, Vandenberg SR, Smith KJ, Cloyd CP, Chang SM, Cha S, et al. MRI apparent diffusion coefficient reflects histopathologic subtype, axonal disruption, and tumor fraction in diffuse-type grade II gliomas. *Neuro Oncol* 2011;13(11):1192–201.
- [8] Barajas RF Jr, Hodgson JG, Chang JS, Vandenberg SR, Yeh RF, Parsa AT, et al. Glioblastoma multiforme regional genetic and cellular expression patterns: influence on anatomic and physiologic MR imaging. *Radiology* 2010;254(2):564–76.
- [9] Barajas RF Jr, Phillips JJ, Parvataneni R, Molinaro A, Essock-Burns E, Bourne G, et al. Regional variation in histopathologic features of tumor specimens from treatment-naïve glioblastoma correlates with anatomic and physiologic MR imaging. *Neuro Oncol* 2012;14(7):942–54.
- [10] Redfield AG. Nuclear magnetic resonance saturation and rotary saturation in solids. *Phys Rev* 1955;98:1787.
- [11] Redfield AG. Nuclear spin thermodynamics in the rotating frame. *Science* 1969;164:1015–23.
- [12] Aronen HJ, Ramadan UA, Peltonen TK, Markkola AT, Tanttu JI, Jääskeläinen J, et al. 3D spin-lock imaging of human gliomas. *Magn Reson Imaging* 1999;17:1001–10.
- [13] Regatte RR, Akella SV, Borthakur A, Kneeland JB, Reddy R. In vivo proton MR three-dimensional T1ρ mapping of human articular cartilage: initial experience. *Radiology* 2003;229:269–74.
- [14] Jokivarsi KT, Hiltunen Y, Grohn H, Tuunanen P, Grohn OHJ, Kauppinen RA. Estimation of the onset time of cerebral ischemia using T1 and T2 MRI in rats. *Stroke* 2010;41(10):2335–40.
- [15] Gröhn OH, Kettunen MI, Mäkelä HI, Penttonen M, Pitkänen A, Lukkarinen JA, et al. Early detection of irreversible cerebral ischemia in the rat using dispersion of the magnetic resonance imaging relaxation time, T1ρ. *J Cereb Blood Flow Metab* 2000;20(10):1457–66.
- [16] Magnotta VA, Heo HY, Dlouhy BJ, Dahdaleh NS, Follmer RL, Thedens DR, et al. Detecting activity-evoked pH changes in human brain. *Proc Natl Acad Sci USA* 2012;109(21):8270–3.
- [17] Borthakur A, Sochor M, Davatzikos C, Trojanowski JQ, Clark CM. T1ρ MRI of Alzheimer's disease. *Neuroimage* 2008;41(4):1199–205.
- [18] Haris M, Singh A, Cai K, Davatzikos C, Trojanowski JQ, Melhem ER, et al. T1ρ (T1ρ) MR imaging in Alzheimer's disease and Parkinson's disease with and without dementia. *J Neurol* 2011;258(3):380–5.
- [19] Markkola AT, Aronen HJ, Paavonen T, Hopsu E, Sipilä LM, Tanttu JI, et al. T1ρ dispersion imaging of head and neck tumors: a comparison to spin lock and magnetization transfer techniques. *J Magn Reson Imaging* 1997;7(5):873–9.
- [20] Poptani H, Duvvuri U, Miller CG, Mancuso A, Charagundla S, Fraser NW, et al. T1ρ imaging of murine brain tumors at 4 T. *Acad Radiol* 2001;8(1):42–7.
- [21] Hakumäki JM, Gröhn OH, Tyynelä K, Valonen P, Ylä-Herttuala S, Kauppinen RA. Early gene therapy-induced apoptotic response in BT4C gliomas by magnetic resonance relaxation contrast T1 in the rotating frame. *Cancer Gene Ther* 2002;9(4):338–45. <http://dx.doi.org/10.1038/sj/cgt/7700450>.
- [22] Kettunen MI, Sierra A, Narvainen MJ, Valonen PK, Ylä-Herttuala S, Kauppinen RA, et al. Low spin-lock field T1 relaxation in the rotating frame as a sensitive MR imaging marker for gene therapy treatment response in rat glioma. *Radiology* 2007;243(3):796–803. <http://dx.doi.org/10.1148/radiol.2433052077>.
- [23] Sepponen RE, Pohjonen JA, Sipponen JT, Tanttu JI. A method for T1ρ imaging. *J Comput Assist Tomogr* 1985;9(6):1007–11.
- [24] Borthakur A, Mellon E, Niyogi S, Witschey W, Kneeland JB, Reddy R. Sodium and T1ρ MRI for molecular and diagnostic imaging of articular cartilage. *NMR Biomed* 2006;19(7):781–821.
- [25] Wheaton AJ, Borthakur A, Kneeland JB, Regatte RR, Akella SV, Reddy R. In vivo quantification of T1ρ using a multislice spin-lock pulse sequence. *Magn Reson Med* 2004;52(6):1453–8.
- [26] Palmer AG, Kroenke CD, Loria JP. Nuclear magnetic resonance methods for quantifying microsecond—millisecond motions in biological macromolecules. *Methods Enzymol* 2001;339:204–38.
- [27] Menezes NM, Gray ML, Hartke JR, Burstein D. T2 and T1ρ MRI in articular cartilage systems. *Magn Reson Med* 2004;51(3):503–9.
- [28] Sage MR. Blood-brain barrier: phenomenon of increasing importance to the imaging clinician. *AJR Am J Roentgenol* 1982;138(5):887–98.
- [29] Gröhn HI, Michaeli S, Garwood M, Kauppinen RA, Gröhn OH. Quantitative T(1ρ) and adiabatic Carr-Purcell T2 magnetic resonance imaging of human occipital lobe at 4 T. *Magn Reson Med* 2005;54:14–9.
- [30] Wheaton AJ, Borthakur A, Reddy R. Application of the keyhole technique to T1ρ relaxation mapping. *J Magn Reson Imaging* 2003;18:745–7.